

SUPPLEMENTARY MATERIAL

Disrupting the Transmembrane Domain Oligomerization of Protein Tyrosine Phosphatase Receptor J Promotes its Activity in Cancer Cells

Elizabeth Bloch^{1¶}, Eden L. Sikorski^{1¶}, David Pontoriero², Bryan Berger², Matthew J. Lazzara², and Damien Thévenin^{1*}

¹Department of Chemistry, Lehigh University (Bethlehem, PA)

²Department of Chemical Engineering, University of Virginia (Charlottesville, VA)

*To whom correspondence should be addressed: damien.thevenin@lehigh.edu

¶These authors contributed equally to this work

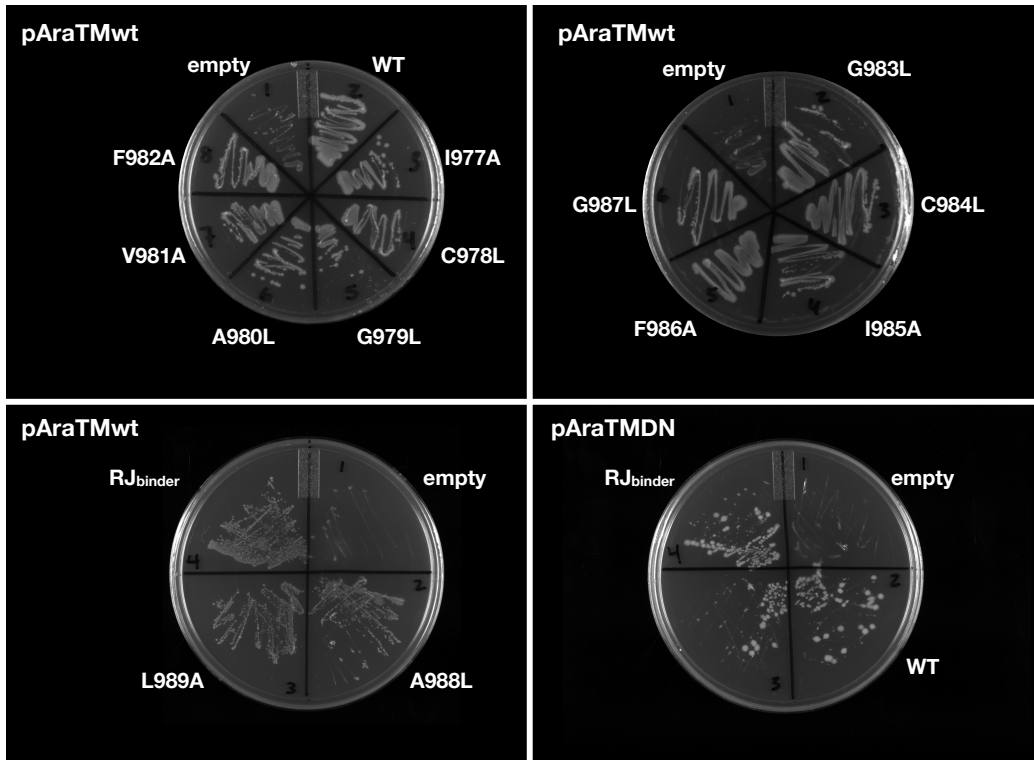


Figure S1. Maltose complementation test. The indicated pAraTMwt or pAraTMDN constructs were transformed into the MBP-deficient *E. coli* strain MM39. Saturated culture from each chimera was streaked onto M9 minimal media plates containing maltose. No growth was observed in the empty vectors, in which no AraC or AraC* fusion is expressed. Recovery of growth was observed for all other fusion constructs, indicating proper orientation in the cell membrane.

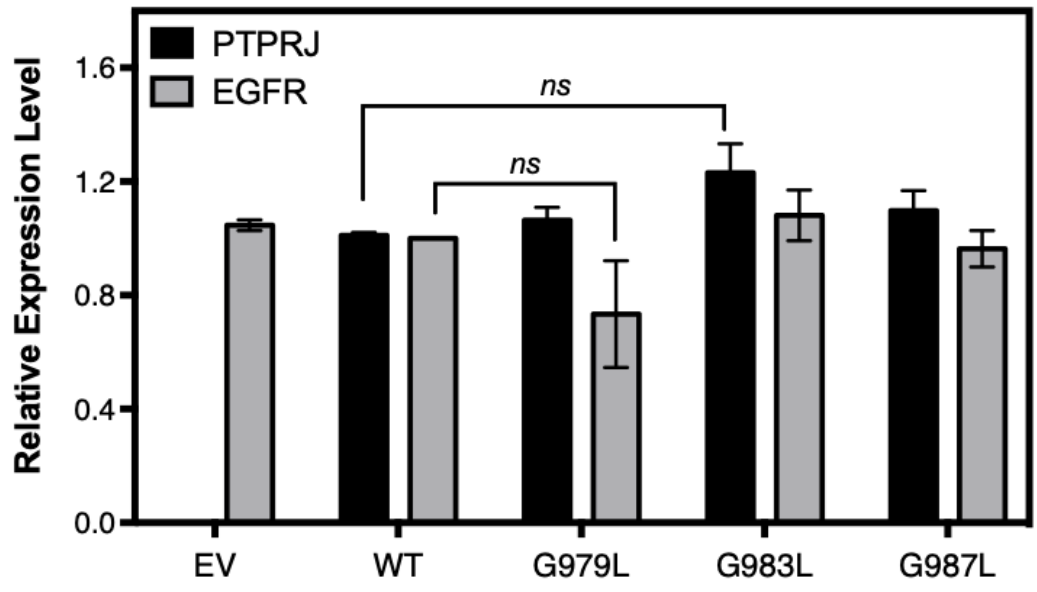


Figure S2. Relative expression levels of total PTPRJ and EGFR in UMSCC2 cells normalized to WT. Results are shown as mean \pm SEM ($n = 3$). Statistical significance was assessed using unpaired t test (at 95% confidence intervals).

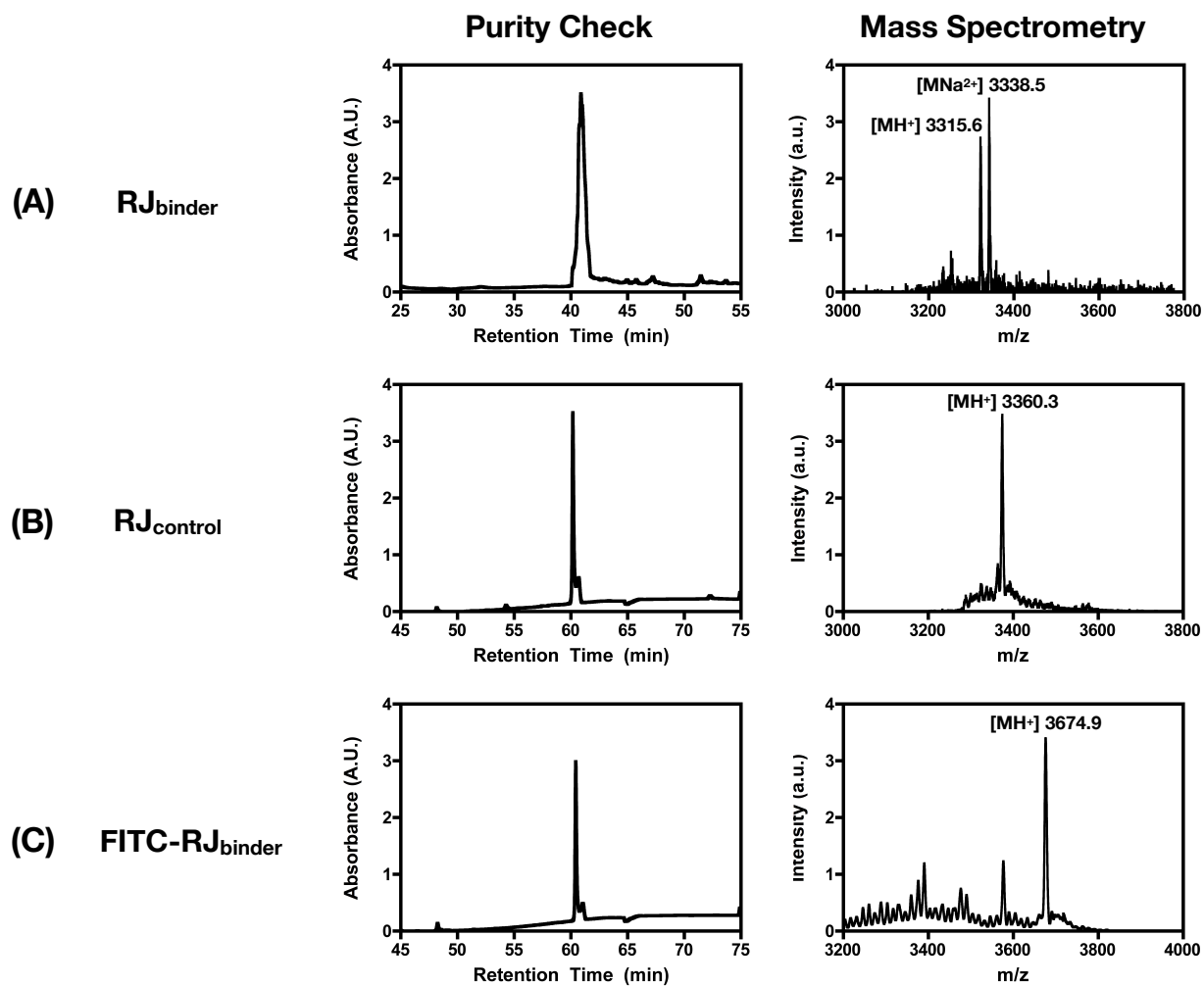


Figure S3. Purity check by RP-HPLC and MALDI-TOF MS spectra of synthesized peptides. **(A)** RJ_{binder} : calculated (MH^+) = 3316.1 g/mol, found (MH^+) 3315.6 g/mol. **(B)** $RJ_{control}$: calculated (MH^+) 3358.2, found (MH^+) = 3360.3 g/mol. **(C)** $FITC-RJ_{binder}$: calculated (MH^+) = 3674.5 g/mol, found (MH^+) = 3674.9 g/mol.

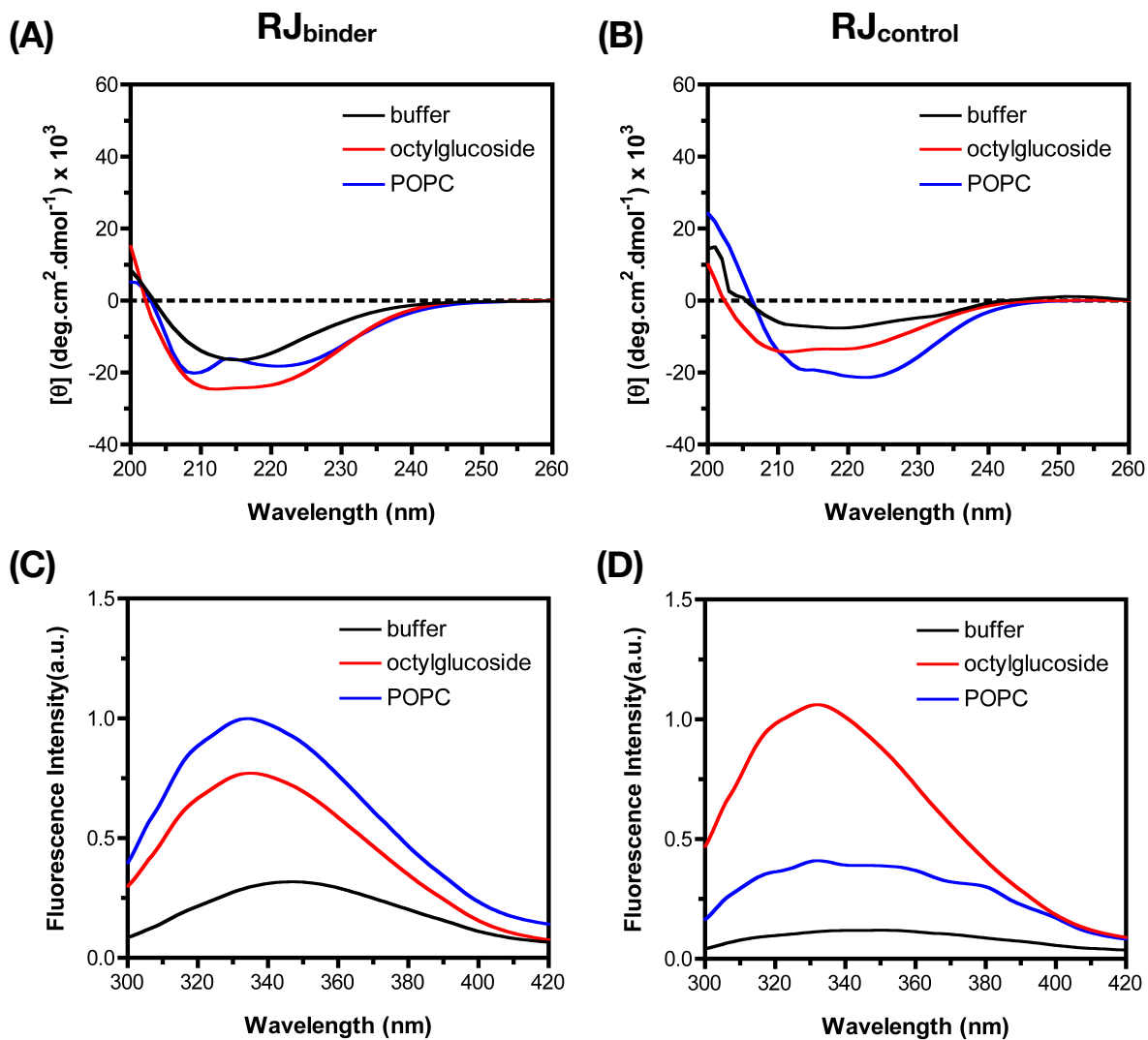


Figure S4. Interaction of RJ_{binder} and $RJ_{control}$ with membrane mimics. Circular dichroism (A,B) and tryptophan fluorescence emission (C,D) of 10 μ M RJ_{binder} and $RJ_{control}$ in buffer (black), 30 mM n-octylglucoside micelles (red) or large unilamellar POPC lipid vesicles at a 1:300 peptide/lipid ratio (blue).

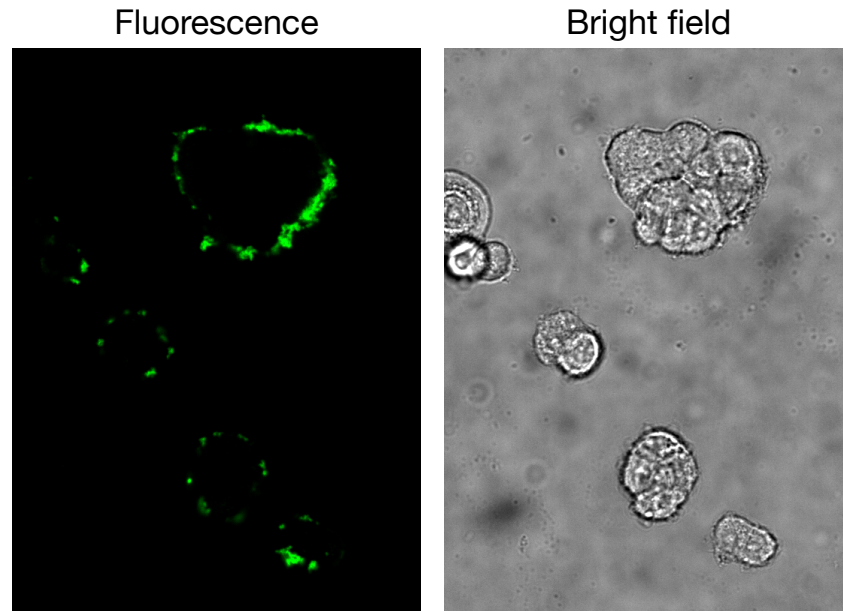


Figure S5. RJ_{binder} partitions into cell membranes. UMSCC2 cells were treated with 10 μ M fluorescently labeled RJ_{binder} reconstituted in n-octylglucoside micelles for 1 h. Representative fluorescence and bright field images taken from spinning disk confocal microscopy are shown.

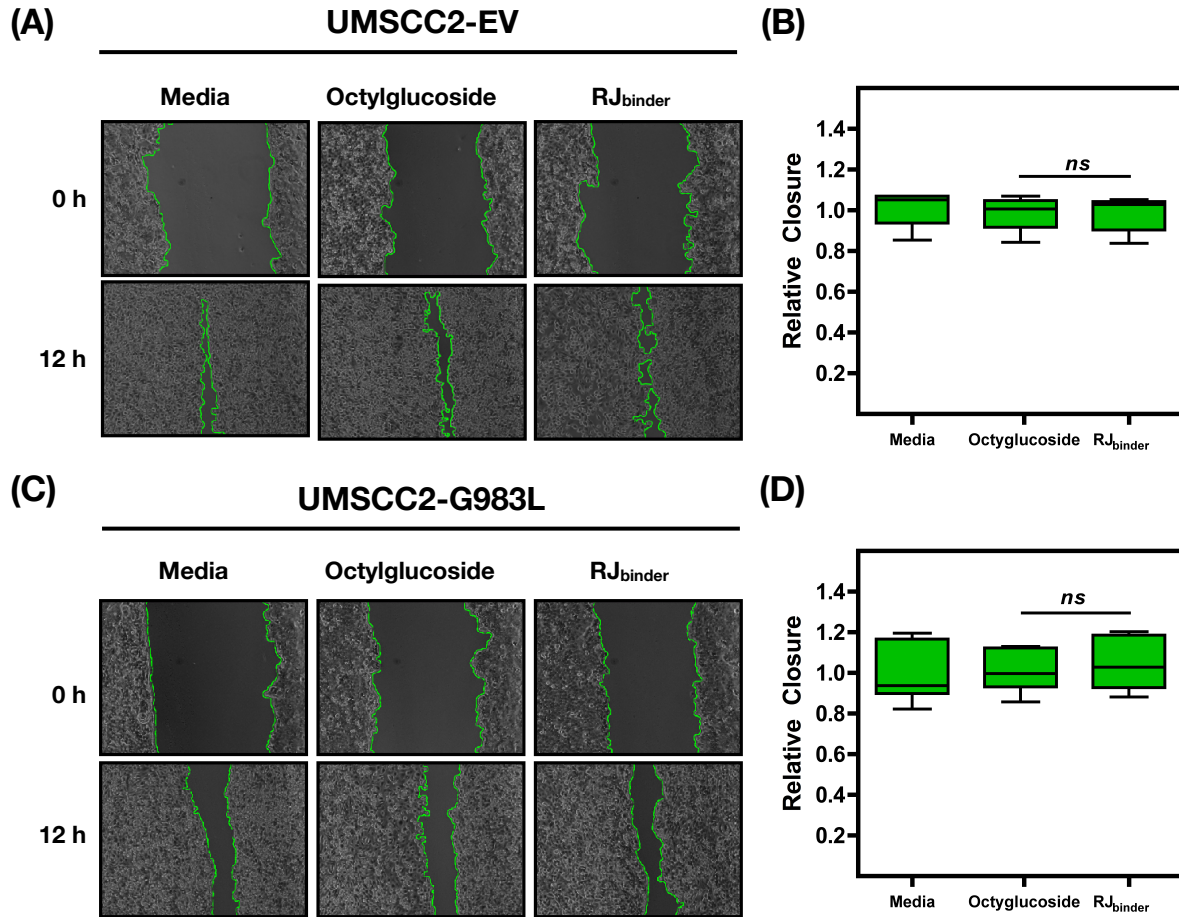


Figure S6. RJ_{binder} has no effect on migration in cells expressing minimal PTPRJ (EV) or the homodimer-disrupting mutant (G983L). Representative phase contrast images with tracings to identify open scratch areas (A,C) and quantification (B,D) of the effect of RJ_{binder} on cells expressing either minimal PTPRJ (A,B) or G983L PTPRJ (C,D). Serum-starved UMSCC2 cells were treated with 10 μ M RJ_{binder} reconstituted in n-octylglucoside micelles for 1 h, scratched (0 h), and incubated media containing EGF (50 ng/mL) for 12 h. Relative closure was quantified by calculating the percent change in area between 0 and 12 h using ImageJ, and then normalized to media containing EGF. (B,D) Results are shown as mean \pm SEM ($n = 6-9$). Statistical significance was assessed using unpaired t test (at 95% confidence intervals).

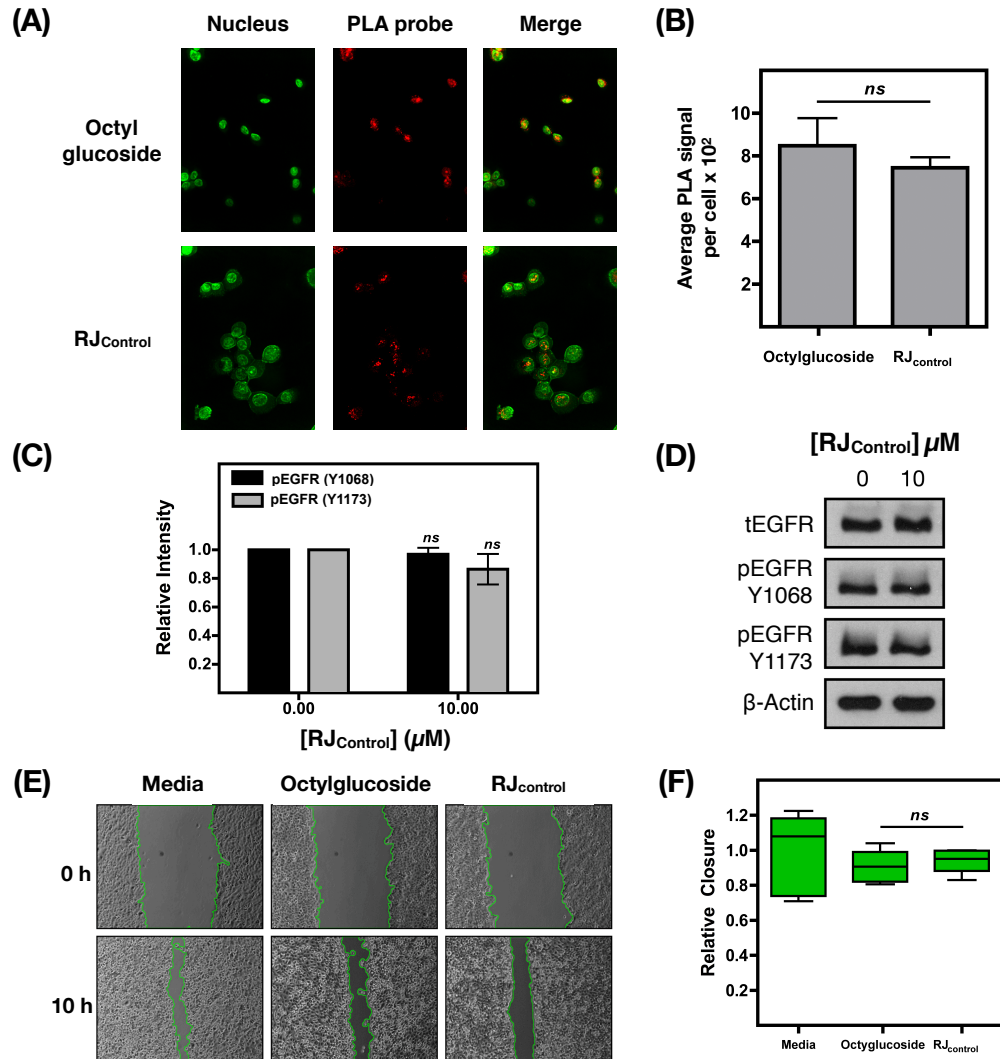


Figure S7. RJ_{control} treatment has no effect on PTPRJ oligomerization, EGFR phosphorylation, or cell migration. (A,B) Representative confocal microscopy images (A) and quantification (B) quantification of the effect of 10 μM RJ_{control} n-octylglucoside micelles on PTPRJ oligomerization using *in situ* PLA. Oligomerization of full-length PTPRJ WT in UMSSC2 cells was measured following treatment with RJ_{control} for 1 h using spinning disk confocal microscopy (green: nucleus; red: PLA for PTPRJ self-association). The average PLA signal intensity per cells was determined using BlobFinder. (B) Results are shown as mean ± SEM ($n > 100$). Statistical significance was assessed using unpaired *t* test (at 95% confidence intervals). (C,D) Quantification (C) and representative immunoblots (D) of the effect of RJ_{control} on EGFR phosphorylation levels. Serum-starved UMSSC2 cells were treated with 10 μM RJ_{control} for 3 h prior to stimulation with EGF. Cell lysates were probed for EGFR and phospho-EGFR (Y1068 and Y1173). The relative (ratio of phosphorylated to total protein) intensities are shown as mean ± SEM ($n = 3$). Statistical significance was assessed using unpaired *t* test (at 95% confidence intervals). (E,F) Representative phase contrast images with tracings to identify open scratch areas (E) and quantification (F) of the effect of RJ_{control} on wound closure. Serum-starved UMSSC2 cells were treated with 10 μM RJ_{control} or 3 mM n-octylglucoside alone for 1 h, scratched (0 h), and incubated in media with EGF (50 ng/mL) for 10 h. Relative closure was quantified by calculating the percent change in area between 0 and 10 h using ImageJ, and then normalized to media containing EGF. (F) Results are shown as mean ± SEM ($n = 6-9$). Statistical significance was assessed using unpaired *t* test (at 95% confidence intervals).

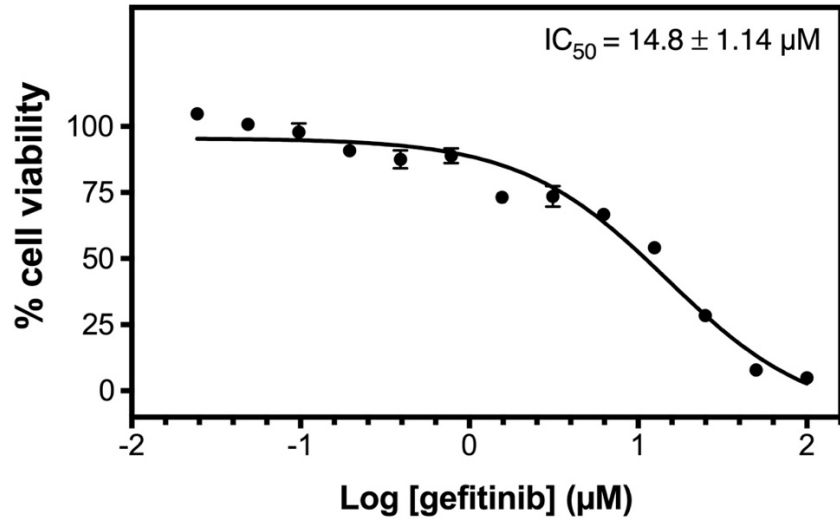


Figure S8. Sensitivity of UMSCC2 cells expressing WT PTPRJ1 towards gefitinib. 5,000 cells/well were treated with increasing concentrations of gefitinib in 1% DMSO for 72 hours. Cell viability was determined using the colorimetric MTT assay. Briefly, 10 µL of a 5 mg/mL MTT stock solution was added to the treated cells and incubated for 2 h at 37 °C. The resulting formazan crystals were solubilized in 200 µL DMSO and the absorbance measured at 580 nm using an Infinite 200 PRO microplate reader (Teca). Results are shown as mean ± SEM ($n = 6$). Data were fitted with a sigmoidal dose-response (Prism for Mac, GraphPad, Inc.).